

**Convergent biochemical pathways for xanthine alkaloid production in plants evolved from ancestral enzymes with different catalytic properties**

Andrew J. O'Donnell<sup>1</sup>, Ruiqi Huang<sup>2</sup>, Jessica Barboline & Todd J. Barkman<sup>3</sup>

Department of Biological Sciences, Western Michigan University, Kalamazoo, MI 49008 United States

<sup>1</sup>Current address: Max Planck Institute for Chemical Ecology, Hans-Knoell-Strasse 8, D-07745 Jena, Germany

<sup>2</sup>Current address: Applied Biomedical Science Institute, 10929 Technology Pl, San Diego, CA 92127, United States

<sup>3</sup>Author for correspondence: Todd J. Barkman: [todd.barkman@wmich.edu](mailto:todd.barkman@wmich.edu)

© The Author(s) 2021. Published by Oxford University Press on behalf of the Society for Molecular Biology and Evolution. This is an Open Access article distributed under the terms of the Creative Commons Attribution Non-Commercial License (<http://creativecommons.org/licenses/by-nc/4.0/>), which permits non-commercial re-use, distribution, and reproduction in any medium, provided the original work is properly cited. For commercial re-use, please contact [journals.permissions@oup.com](mailto:journals.permissions@oup.com)

## Abstract

Convergent evolution is widespread but the extent to which common ancestral conditions are necessary to facilitate the independent acquisition of similar traits remains unclear. In order to better understand how ancestral biosynthetic catalytic capabilities might lead to convergent evolution of similar modern-day biochemical pathways, we resurrected ancient enzymes of the Caffeine Synthase (CS) methyltransferases that are responsible for theobromine and caffeine production in flowering plants. Ancestral CS enzymes of *Theobroma*, *Paullinia* and *Camellia* exhibited similar substrate preferences but these resulted in the formation of different sets of products. From these ancestral enzymes, descendants with similar substrate preference and product formation independently evolved after gene duplication events in *Theobroma* and *Paullinia*. Thus, it appears that the convergent modern-day pathways likely originated from ancestral pathways with different inferred flux. Subsequently, the modern-day enzymes originated independently via gene duplication and their convergent catalytic characteristics evolved to partition the multiple ancestral activities by different mutations that occurred in homologous regions of the ancestral proteins. These results show that even when modern-day pathways and recruited genes are similar, the antecedent conditions may be distinctive such that different evolutionary steps are required to generate convergence.

## Introduction

The ubiquity of convergent trait acquisition throughout the tree of life suggests that evolution may be, at least to some extent, repeatable due to some combination of constraint on one hand and strength of natural selection, on the other (Storz 2016). One framework by which to conceptualize and study mechanisms of convergence emphasizes dissection of the biological hierarchy through study of the pathways (biochemical or developmental), underlying genes, encoded protein functions, and mutational paths involved (Des Marais and Rausher 2010; Manceau et al. 2010; Losos 2011). At one end of the spectrum, convergent traits may arise from different pathways, genes and sets of mutations whereas at the other, in principle, it is possible to have the same pathway generate a similar phenotype in independent lineages that is realized by orthologous genes that acquired their novel functions by identical mutations to the same ancestral nucleotides (Zhang 2006; Christin et al. 2010; Manceau et al. 2010; Storz 2016)□. While convergent evolution has been studied in terms of the underlying modern-day pathways and genes recruited, the ancient underpinnings of the independent origins of traits are less well understood. For instance, in the case of convergently evolved metabolites generated by the same biosynthetic pathways, (Pichersky and Lewinsohn 2011) ancestral biochemical flux may or may not have been the same as that exhibited by modern-day descendant species. Computational models indicate that evolutionary changes in pathway flux may be predictable and are influenced by biochemical network structure, gene expression levels and kinetic properties of the enzymes involved (Wheeler and Smith 2019). One way to investigate the historical sequence of independent pathway evolution involves ancestral sequence resurrection (ASR) (Thornton 2004; Dean and Thornton 2007) which provides an experimental means to directly determine the genetic and biochemical changes leading to convergence (Zhang 2006; Natarajan et al. 2016). This experimental method has provided novel insight into protein functional evolution in several different systems (Chang et al. 2002; Bridgham et al. 2006; Gaucher et al. 2008; Bridgham et al. 2009; Field and Matz 2010; Smith et al. 2012; Lichman et al. 2020). Utility of ASR was shown to be particularly valuable for revealing ancestral changes to enzymes involved in the corticosteroid pathway that allowed for biosynthetic elaboration in primates (Olson-Manning 2020).

One example of convergent trait evolution in angiosperms is the biosynthesis of xanthine alkaloids, like caffeine, which have several ecological roles (Suzuki and Waller 1987; Baumann et al. 1995; Ashihara and Crozier 2001; Uefuji et al. 2005; Anaya et al. 2006; Wright et al. 2013)□□. Caffeine (CF) is produced in various plant tissues via the sequential methylation of xanthine alkaloid precursors by either caffeine synthase (CS) or xanthine methyltransferase (XMT) enzymes which are paralogs in the SABATH family of S-adenosyl-L-methionine (SAM)-dependent methyltransferases (Suzuki and Takahashi 1976; Mazzafera et al. 1994; Ashihara et al. 1996;

Mizuno, Kato, et al. 2003; Kato and Mizuno 2004) (Fig. 1; Fig. S1). *Coffea* spp. (coffee) and *Citrus sinensis* (citrus) convergently utilize XMT enzymes to produce caffeine (Uefuji et al. 2003; McCarthy and McCarthy 2007; Denoeud et al. 2014; Huang et al. 2016)(Fig. S1). Yet, these orthologous enzymes catalyze divergent pathways; primarily via xanthosine (XR), 7-methylxanthine (7X), and theobromine (TB) in *Coffea*, and xanthine (X), 1- and 3- methylxanthine (1X, 3X), and theophylline (TP) in *Citrus* (Fig. 1). The pathway in *Camellia sinensis* (tea) is thought to be convergent with *Coffea*, even though it recruited CS enzymes to catalyze the same reactions (Kato et al. 2000) (Fig. 1; Fig. S1). *Paullinia cupana* (guarana) and *Theobroma cacao* (cocoa) convergently utilize CS-type enzymes to methylate xanthine alkaloids as in *Camellia* (Huang et al. 2016) (Fig. S1). However, the CS enzymes of *Paullinia* and *Theobroma* primarily convert X to 3X and 3X to TB (Fig. 1). Surprisingly, the CS1 enzymes in *Paullinia* and *Theobroma* that convert X to 3X appear to have evolved independently after gene duplication, as have their CS2 enzymes which catalyze the conversion of 3X to TB (Huang et al. 2016). A CS-type enzyme has been reported to convert TB to CF in *Paullinia* but none is yet known for *Theobroma* (Schimpl et al. 2014; Huang et al. 2016)(Fig. 1). The multiple modern-day CS enzymes in *Paullinia*, *Theobroma* and *Camellia* are part of an ancient lineage but, like the XMT enzymes of *Coffea* and *Citrus*, arose by independent duplication in each caffeine-producing group more recently (Huang et al. 2016)(Fig. S1).

Individual CS or XMT enzymes may generate considerable biochemical complexity due to their potential to 1) methylate multiple substrates in the pathway and 2) produce multiple products from single substrates due to methylation of different ring N atoms (see N1, N3 or N7 in Fig. 1) (Kato et al. 2000; McCarthy and McCarthy 2007; Huang et al. 2016). This enzymatic complexity, combined with the fact that intermediates in the pathway do not accumulate to appreciable levels, makes it difficult to determine for any one species if flux is linear or highly branched throughout the metabolic network shown in Fig. 1. Nonetheless, primary routes to caffeine biosynthesis have been hypothesized based a combination of documented gene co-expression patterns, enzyme substrate preferences and detection of intermediate metabolites in metabolomic and radioisotope tracer studies (Kato et al. 1996; Mizuno, Okuda, et al. 2003; Uefuji et al. 2003; Kato and Mizuno 2004; Ashihara et al. 2008; Huang et al. 2016; Deng et al. 2020). Angiosperm CS- and XMT-type enzymes have been characterized mainly from caffeine-producing species; yet, orthologs are known from other non-xanthine alkaloid accumulating relatives (Huang et al. 2016). In these cases, it is unclear why the genes would have been maintained over long periods of time if they weren't involved in caffeine biosynthesis. In *Mangifera*, the only non-caffeine-producing species studied, it was shown that benzoic acid is the preferred substrate for its XMT ortholog with no xanthine alkaloid activity detected. Benzoic and salicylic acid methylation was also shown for the ancestral

angiosperm XMT protein which suggests that xanthine alkaloid methylation only recently evolved in descendant enzymes (Huang et al. 2016).

The convergent xanthine alkaloid pathways in *Paullinia* (Sapindales) and *Theobroma* (Malvales) catalyzed by recently and independently duplicated orthologous CS enzymes makes this a remarkable case of convergence because they are members of lineages that diverged at least 60 million years ago (Huang et al. 2016; Zeng et al. 2017). As they have both converged on the use of orthologous proteins to catalyze the same pathway, we predict that each lineage would have possessed progenitor enzymes with similar catalytic properties that would allow for evolution of the modern-day pathway following the same biochemical steps from X to 3X to TB. Furthermore, it has been demonstrated that single amino acid substitutions within the predicted active site in XMT enzymes were sufficient for specialization on xanthine alkaloid substrates in the *Citrus* lineage (Huang et al. 2016). Therefore, we predict that mutations leading to changes in substrate preference of CS enzymes are also constrained to the same active site regions in spite of their ancient divergence. In this study, we resurrected ancestral enzymes at key branching points of the CS lineage to test these predictions.

## Results & Discussion

### *Evolution of theobromine and caffeine production in Paullinia, Theobroma, and Camellia originated from ancestral CS enzymes with similar substrate preferences to form distinct sets of products*

Even though whole genome sequences were queried, CS orthologs appear to be lacking from most asterid lineages like Lamiales & Solanales and seem to be encoded in only a scattered set of angiosperm lineages as shown in Fig. 2A (see also Fig. S2). The only functionally characterized CS enzymes are known from Sapindales, Malvales and Ericales. These are also the only lineages from which xanthine alkaloids (caffeine or precursors) are reliably known of those shown in Fig. 2A (Ashihara and Suzuki 2004). Thus, it is unclear what the activity of CS orthologs from Myrtales, Geraniales and Cornales may be since none of their proteins have been functionally characterized. One potential role for the orthologs from these lineages is trigonelline biosynthesis which also requires ring nitrogen methylation and has been shown for an XMT-type enzyme in *Coffea* (Mizuno et al. 2014). Alternatively, it may be that CS enzymes in all of the lineages shown in Fig. 2A are involved in xanthine alkaloid biosynthesis to produce caffeine at low, difficult-to-detect levels. If so, the distribution of this important stimulant could be much more widespread in angiosperms than is currently appreciated.

To investigate the characteristics of ancient CS-type enzymes in angiosperms, we experimentally resurrected and characterized at least two ancestral allelic variants for each of the progenitors predicted for *Paullinia* (PcAncCS1), *Theobroma* (TcAncCS1) and *Camellia* (CsAncCS) (Figure 2C-E nodes M, O, & Q; Fig. S1; Fig. S3-5). Surprisingly, all three of these ancestral enzymes had highest relative activity with 7X even though preference for the substrate is not exhibited by the modern-day CS1 & CS2 enzymes derived from each of them (Figure 2C-E; Fig. S3-5). This similar methylation activity was exhibited in spite of a substantial degree of sequence divergence amongst these ancestral CS enzymes which ranges from 51-63%. All three ancestral enzymes converted 7X to TB by methylation at N3 but in addition, TcAncCS1 and CsAncCS converted 7X to paraxanthine (PX) by methylation at the N1 position (Fig. 2C-E; Table S1). Each ancestral enzyme also had lower relative activity with X: in PcAncCS1, X was converted to 3X while TcAncCS1 and CsAncCS methylated X to produce both 1- and 3X (Fig. 2C-E; Table S1). The product of the reaction with 3X was below our detection limit for PcAncCS1 and CsAncCS but in TcAncCS1, 3X was converted to TP (Fig. 2D, Table S1). Thus, N1 and N3 methylation were properties of these ancestral enzymes but none appear to methylate the N7 position of any substrate we tested.

Since each of the ancestral enzymes in the *Paullinia*, *Theobroma* and *Camellia* lineages appears to have been capable of converting xanthine to a monomethylated product (1X & 3X) (Fig. 2C-E), they may have provided the beginnings of the modern-day caffeine biosynthetic pathways. This is predicted under the Cumulative Hypothesis for pathway evolution in which earlier steps are predicted to evolve first (Granick 1957; Huang et al. 2016); in addition, TcAncCS1 could also have formed the dimethylated product, TP. If these molecules were to accumulate in ancestral plant tissues, they could have conferred a selective advantage which would likely result in retention of the ancient genes because 1X & 3X have been shown to bind to modern-day rat adenosine receptors (Daly et al. 1983) and TP can modulate Adenylate Cyclase in insects (Nathanson 1984). Their formation in tissues is tenable since PcAncCS1 and TcAncCS1 have apparent  $K_M$  estimates for X that are comparable to modern-day CS enzymes (53-417  $\mu\text{M}$ ) (Table 1)(Huang et al. 2016). Alternatively, if ancestral X methylation was not physiologically relevant, then their high 7X activity was probably fortuitous since ancestral plants would not likely accumulate 7X to react with, unless other enzymes were responsible for its production. Yet, only modern-day CS and XMT-type enzymes have been demonstrated to produce 7X making it unlikely that the substrate was produced in ancient plant tissues (Mizuno, Okuda, et al. 2003; Uefuji et al. 2003; Huang et al. 2016). In this case, these enzymes would have been exapted for their modern-day roles in theobromine and caffeine biosynthesis because N3 methylation of 7X to form TB in *Camellia* CsAncCS appears to be an ancient characteristic that has been maintained over 100 my and is utilized as an enzymatic

step for modern-day caffeine production (Kato et al. 2000) (Fig. 1 & 2E). Even if CS genes were maintained for some alternative function outside of xanthine alkaloid methylation that we have not assayed for, it is apparent that ancestral 7X preference is an enzymatic characteristic also maintained by modern-day CS-type enzymes in non-caffeine accumulating *Camellia* species (Ishida et al. 2009) and *Theobroma* (Yoneyama et al. 2006) which appears to contribute to TB formation.

Although each of the ancestral enzymes catalyzed a unique set of xanthine alkaloid products, *Paullinia* and *Theobroma* ultimately evolved convergent pathways to TB biosynthesis (Fig. 1; Fig. 2C & D) (Huang et al. 2016). At a minimum, this would have required independent acquisition of N7 methylation of 3X by *Paullinia* and *Theobroma* CS enzymes in order for them to produce TB, the second metabolite in the pathway towards caffeine (Fig. 1; Fig. 2C & D). To establish how this change to xanthine alkaloid metabolism occurred, we resurrected and experimentally characterized the younger ancestral enzymes that descended from PcAncCS1 and TcAncCS1 and ultimately gave rise to the specialized modern-day CS1 and CS2 paralogs independently in *Paullinia* and *Theobroma*.

### ***Convergent duplication events of Paullinia and Theobroma ancestral CS enzymes allowed for a connected pathway to TB biosynthesis through convergent catalytic changes***

Gene duplication of PcAncCS1 in the *Paullinia* CS lineage (Node M) gave rise to PcAncCS2 (Node N) and a modern-day descendant, *Paullinia* “CS-like”, for which no enzymatic activity was detected (Fig. 2C). In both allelic variants of PcAncCS2, as in the ancestor PcAncCS1, activity with 7X was still highest to form TB and PX while methylation with X to form 3X remained relatively low; however, in this descendant, higher relative activity with 3X evolved to form TB by N7 methylation (Fig. 2C Node N; Fig. S6; Table S1). As a result, this change would have allowed for extension of the caffeine pathway by sequential methylation from the ancestral step of X to 3X to include 3X to TB in a manner consistent with the Cumulative Hypothesis which predicts that later evolved biosynthetic steps build upon earlier ones within a pathway (Granick 1957).

In *Theobroma*, duplication of TcAncCS1 at Node O led to the evolution of TcAncCS2 (Node P) as well as *Theobroma* BTS (Fig. 2D). Whereas BTS retained ancestral preference to methylate 7X (Yoneyama et al. 2006), both allelic variants of TcAncCS2 suggest it lost ancestral preference for 7X and evolved highest relative activity with X, converting it solely to 3X (Fig. 2D; Fig. S7; Table S1). This result represents specialization for N3 methylation due to loss of N1 activity with xanthine. TcAncCS2 also converted 3X to TB, which required acquisition of N7 methylation and loss of N1 methylation of the substrate (Fig. 2D; Table S1). Thus, both *Theobroma* and *Paullinia* ancestral enzymes acquired N7 methylation of 3X following the earliest

known duplications that occurred in each lineage (Fig. 2C & D). As these independent gene duplication events gave rise to descendant enzymes capable of performing the sequential methylation steps required to convert X to TB, they could be viewed as convergent changes that facilitated the evolution of the same pathway steps in both lineages. In the case of *Theobroma*, it appears that the first two biochemical steps catalyzed by its modern-day enzymes evolved by a diversion away from ancestral flux to 1X from X and TP from 3X as seen in TcAncCS1 to primarily X to 3X to TB, rather than being gradually assembled one reaction at a time as in *Paullinia* (Fig. 2C & D).

The restructuring of relative substrate preferences and methylation patterns observed in TcAncCS2 (Fig. 2D) prompted further investigation into its kinetic properties as well as those of TcAncCS1 from which it descended; it was not clear if the relative preference shift towards X activity in TcAncCS2 was due to higher affinity for it, or merely a relative loss in recognition of other substrates. The Michaelis-Menten kinetic parameter estimates summarized in Table 1 indicate that TcAncCS2 had a  $k_{cat}/K_M$  of  $82.1 \text{ s}^{-1} \text{ M}^{-1}$  with X which is 37-fold higher than 3X (and likely that of 7X for which activity was too low to determine kinetic parameters), while in TcAncCS1, the  $k_{cat}/K_M$  with X was comparable to that of 3X but 4 times lower than 7X (Table 1). The apparent improvement of TcAncCS2 with xanthine relative to other substrates was concomitant with a switch away from N1 towards N3 methylation and appears to have set ancestral flux into the beginning of the pathway to TB and CF via 3X predicted for modern-day *Theobroma* (Huang et al. 2016). However, even though TcAncCS2 evolved to perform the two successive enzymatic steps to TB, kinetic estimates predict that flux may have been low for this single ancestral enzyme. The  $k_{cat}/K_M$  for TcAncCS2 with 3X, the product of the reaction with X and second substrate in the pathway to TB, was estimated to be  $2.2 \text{ s}^{-1} \text{ M}^{-1}$  (Table 1). Because the specificity constant of TcAncCS2 for 3X is nearly 40 times lower than that of xanthine, from which it is biochemically derived, the conversion of 3X to TB is predicted to have been low in the presence of this single ancestral enzyme, unless cellular concentrations of X were to become depleted.

After the origin of PcAncCS2 by duplication from PcAncCS1, it was subsequently duplicated again resulting in the evolution of one descendant, PcCS1, that acquired near-complete preference for X to form 3X and a second descendant, PcCS2, that evolved specificity for 3X to form TB (Huang et al. 2016)(Fig. 2C). Likewise, initial gene duplication of TcAncCS1 gave rise to TcAncCS2; this daughter gene was then duplicated later to result in modern-day TcCS1, which prefers to methylate X to form 3X, and TcCS2, which prefers to methylate 3X to form TB (but also has lower relative activity with X to form 7X) (Huang et al. 2016)(Fig. 2D). These independent duplications in the two lineages therefore represent additional convergence between *Paullinia* and *Theobroma* at the level of genes involved; it wasn't until the duplications of PcAncCS2 and



TcAncCS2 that paralogs with the same substrate preferences emerged in the two lineages. In both cases, this likely resulted in a more catalytically favorable pathway from X to 3X to TB. Although we were not able to estimate kinetic parameters for PcAncCS2 due to low protein yields after purification, kinetic parameters of TcAncCS2 and its descendant enzymes predict that specialists would be favored as 3X would not compete for active site binding; the same is perhaps true for *Paullinia* enzymes.

### ***Divergent mutations to homologous protein regions facilitated convergent shifts towards substrate specialization in Paullinia and Theobroma***

In *Paullinia* and *Theobroma*, alignments show that Region I (Fig. 3A) was mutated in both CS enzyme lineages and is predicted to interact with substrate molecules within the active site, as defined by the *Coffea* XMT and *Clarkia* SAMT crystal structures as well as mutagenesis of *Citrus* XMT (Zubieta et al. 2003; McCarthy and McCarthy 2007; Huang et al. 2016). Within Region I of the *Paullinia* CS lineage, Thr25 of PcAncCS2 (Node N) was replaced by Ser in modern-day PcCS2 (Fig. 2C & 3A). Experimental replacement of Thr25 by Ser in PcAncCS2 largely recapitulated the enzymatic shift towards 3X preference to form TB as in its descendant, PcCS2, and caused loss of nearly all ancestral activity with other substrates (Fig. 2C & 3B; Table S1). Within the *Theobroma* lineage leading from TcAncCS2 (Node P) to modern-day TcCS2, Region I was substituted such that SAG21-23 was replaced by AEA (Fig. 2D & 3A). Experimental mutation of the three contiguous sites resulted in a convergent shift of relative preference for 3X to form TB, like was shown in the *Paullinia* lineage, as well as the ability to convert X to 7X making the mutant very similar to modern-day TcCS2 (Fig. 2D & 3B; Table S1). Thus, convergent improvement to 3X methylation of the N7 position occurred by divergent mutations to different codons of a broadly homologous region of CS-type enzymes. Support for the hypothesis that Region I is necessary for xanthine alkaloid methylation specificity is further strengthened by the fact that a convergent amino acid replacement to that of PcAncCS2 occurred in the XMT lineage of *Citrus* caffeine biosynthetic enzymes (Huang et al. 2016)(Fig. 3A). In this case, instead of T25S as inferred for *Paullinia* PcAncCS2, Pro25 was replaced by Ser in CisAncXMT2 and this also resulted in improved activity with 3X (Huang et al. 2016). However, although P25S increased activity with 3X in CisAncXMT2, this improved upon N1 methylation and resulted in the loss of N7 methylation unlike the case for PcAncCS2 in which N7 activity increased when Ser replaced Thr in the presumed active site. Thus, this convergent amino acid replacement by Ser in these SABATH paralogs did not result in the evolution of convergent catalytic properties.

Amino acid replacements in Region III in both the *Paullinia* and *Theobroma* ancestral CS lineages, also produced similar convergent effects on substrate preference. In *Paullinia*, Asn307 of

PcAncCS2 was mutated to Tyr in modern-day PcCS1 which shows near-complete preference for X to form 3X (Fig. 2C & 3A). When we experimentally replaced Asn307 with Tyr in PcAncCS2, all activity with 3- and 7X was lost such that specialization for xanthine methylation at N3 resulted (Fig. 3B; Table S1). Therefore, this single replacement largely recapitulated the evolution of enzyme substrate preference of PcCS1 (Fig. 2C & 3B). TcAncCS2 descended from TcAncCS1 and switched substrate preference from 7X to X. TcAncCS2 differs from its ancestor by three amino acids in Region III (Fig. 3A). When we experimentally replaced Asn307, Leu308, and Ser310 of TcAncCS1 by Gly307, His308, and Cys310 (NLRS307-310GHRC), the mutant showed higher activity with X to produce 3X, much like TcAncCS2, (although it also formed 1X) (Fig. 3B; Table S1). Thus, convergence towards N3 methylation of X appears to have evolved in part by different substitutions to the same homologous protein Region III.

Collectively, our results show that the ancient pathways to methylate xanthine alkaloids in *Paullinia* and *Theobroma* ancestors likely differed from the similar ones used by species today. Because the pathways later converged it suggests that selection may be important for pathway flux changes over time. After subsequent gene duplication and divergence, single ancient enzymes alone could perform the pathway steps that the multiple modern-day descendants currently catalyze. That convergence subsequently resulted from independent gene duplication events that led to the partitioning of the same biochemical reactions in two enzymes in each of the two lineages studied is remarkable. These results suggest that two modern-day enzymes are better than one ancestral enzyme in terms of pathway flux and product accumulation which is largely consistent with predictions under a model of escape from adaptive conflict (Des Marais and Rausher 2008) although a rigorous test of this model was beyond the scope of this study (Barkman and Zhang 2009). Similar to the CS enzymes we have studied, ancestral constraints for multistep enzymes in the corticosteroid pathway were shown to be at least partly alleviated after gene duplication in primates (Olson-Manning 2020). Although it appears that the modern-day duplicated CS enzymes are co-expressed in *Paullinia* and *Theobroma* (Huang et al. 2016), knowledge of ancestral tissue-specific expression patterns for these enzymes would further understanding of the mechanisms of convergence; however, such data are difficult to infer with precision due to our lack of knowledge of ancestral transcriptional regulators and *cis*-regulatory elements. Finally, because we show that different mutations to homologous sequence regions led to convergence, constraint on the mutational paths available to each lineage is implicated. Future work aimed at testing the relative roles for selection and constraint for this and other cases of convergence may benefit from the use of ancestral sequence resurrection that can reveal evolutionary aspects of the process that may not have been predicted a priori.

## Materials & Methods

### Phylogenetic analyses

In order to accurately determine the orthology of *Paullinia* (Sapindales), *Theobroma* (Malvales) and *Camellia* (Ericales) xanthine alkaloid-producing enzymes, amino acid sequences from all previously characterized SABATH gene family members and those from various land plant complete genomes were obtained from GenBank and the PlantTribes database (Wall et al. 2008). We also queried the OneKP database in order to provide more detailed branching relationships of the recently evolved CS enzymes of *Paullinia*, *Theobroma* and *Camellia* as shown in Fig. S1. Alignment of amino acid sequences was achieved using MAFFT version 7 (Kato and Standley 2013) using the auto search strategy to maximize accuracy and speed. A maximum likelihood phylogenetic estimate for the SABATH family members was obtained using PhyML (Guindon et al. 2010) assuming the JTT model for amino acid substitution with an invariant and gamma parameter for among-site rate heterogeneity as determined by ProtTest (Abascal et al. 2005). Bootstrap support was evaluated based on 100 pseudoreplicated datasets.

### Ancestral sequence resurrection and mutagenesis

Ancestral enzyme sequences for nodes M–Q were estimated from the full CS lineage of the SABATH gene family shown in Fig. 2B using the JTT+ Gamma model of amino acid substitution as implemented in Codeml of PAML 4.0 (Yang 2007). Importantly, where possible, we relied on a combination of genomic sequence as well as supporting transcriptomic data to ensure that high-quality sequence was analyzed in order to avoid introducing potential sequence artifacts into our ancestral state estimates. This was possible for *Theobroma* and *Camellia* (Argout et al. 2008; Argout et al. 2011; Taniguchi et al. 2012; Wei et al. 2018); however, no genome exists for *Paullinia* so in that case we relied on transcriptome data alone (Angelo et al. 2008; Figueiredo et al. 2011) as reported in Huang et al., 2016. Alignments of the ancestral proteins with their modern-day descendants are shown in Fig. S8. In order to determine ancestral protein lengths in regions with alignment gaps, we coded each sequence for the number of amino acids possessed and used parsimony to determine ancestral residue numbers as in our previous studies (Huang et al. 2012; Huang et al. 2016). The estimated sequences were synthesized by Genscript Corp. and had codons chosen for optimal protein expression in *E. coli*. For sites that had relatively low posterior probabilities or that differed when the gamma parameter was not assumed, we generated alternative ancestral alleles by site-directed mutagenesis using the QuickChange® Site-Directed Mutagenesis Kit (Agilent), following the manufacturer's protocol. This allowed us to assess whether experimentally determined enzyme activities were dependent upon particular amino acid

reconstructions. At least two ancestral enzymes were characterized for each node M-Q in Fig. 2 even though average posterior probabilities were high for most sites (see average site-specific posterior probabilities in Fig. S3-S7). Details of those alternative alleles are provided in Fig. S3-S7 including which sites were mutated as well as individual enzyme activity of each allele. Assays for each node were obtained for at least two alleles and mean relative activity with each substrate is shown in the pie charts of Fig. 2C-E.

### Cloning, heterologous expression and purification of enzymes

Ancestral gene sequences were synthesized by Genscript and were subcloned from the pUC57 cloning vector into the pET-15b (Novagen) expression vector. Plasmid DNA was first digested at 37° C for 6 hours using 1.5 µg of DNA and NdeI and BamHI in 30 µl reactions. Linear fragments corresponding to the expected sizes were gel purified using the QIAEXII gel extraction kit (Qiagen Corp.) according to the manufacturer's instructions. Purified DNA fragments were ligated into pET15b using T4 DNA ligase from New England Biolabs. Reactions were incubated at 16° C overnight. Ligation products were transformed into Top10 *E. coli* cells using 2 µl of ligation reaction. Minipreps of positive transformants were obtained using a Qiaprep spin miniprep kit (Qiagen Corp.). 10 ng of each plasmid was used to transform and grow BL21 *E. coli* cells using standard plating and incubation methods. Induction of His<sub>6</sub>-protein was achieved in 50 ml BL21 (DE3) cell cultures with the addition of 1mM IPTG at 23° C for 6 hours as described previously (Huang et al. 2016). Purification of the His<sub>6</sub>-tagged protein utilized TALON spin columns (Takara Bio) and followed the manufacturer's instructions. Bradford assays were used to determine purified protein concentration and recombinant protein purity was evaluated on SDS-PAGE gels. The plasmids used to produce ancestral proteins are freely available upon request.

### Enzyme Assays

All enzymes were tested for activity with the eight xanthine alkaloid substrates shown in Figure 1. Radiochemical assays were performed in 50 µl reactions with 0.01 µCi (0.5 µl) <sup>14</sup>C-labeled SAM, 100 µM methyl acceptor substrate dissolved in 0.5 M NaOH and 10-20 µl purified protein in 50 mM Tris-HCl buffer at 24° C for 60 minutes. Negative controls were composed of the same reagents except that the methyl acceptor substrate was omitted and 1 µl of 0.5 M NaOH was added instead. Methylated products were extracted in 200 µl ethyl acetate and quantified using a liquid scintillation counter. The highest enzyme activity reached with a specific substrate was set to 1.0 and relative activities with remaining substrates were calculated. Each assay was run at least twice so that mean, plus standard deviation, could be calculated as shown in Fig. S3-7. Although the enzymes in this study did not show high activity with some of the substrates (eg. 1X, XR), we do

not believe this is due to any artifact or limitation of the assays since our previous studies using the same conditions did detect catalysis of those structures (Huang et al. 2016).

### Enzyme kinetics

Kinetic parameters ( $k_{\text{cat}}$  and  $K_M$ ) of the methyltransferases with a given substrate were determined using the 50  $\mu\text{l}$  radioactive assay described above. However, appropriate enzyme concentration and incubation time were determined in time-course assays with low non-saturating substrate concentrations to ensure that the reaction velocity was linear during the assay period. When varying xanthine alkaloid substrate concentration, the SAM concentration was held constant and saturated at 320  $\mu\text{M}$ . Assays were run in duplicate and initial velocities versus substrate concentration were plotted using GraphPad Prism (GraphPad Software, La Jolla, CA) to fit the hyperbolic Michaelis-Menten equation to calculate  $V_{\text{max}}$  and  $K_M$ .  $V_{\text{max}}$  was converted to  $k_{\text{cat}}$  based on estimated protein concentrations and expressed in units of  $\text{s}^{-1}$ .

### Liquid Chromatography – Tandem Mass Spectrometry (LC-MS/MS)

LC-MS tandem mass spectrometry was used to confirm product identity from ancestral enzyme assays. Detection was optimized using pure standards for the expected products diluted to 1  $\mu\text{M}$  in 0.1% formic acid/50% acetonitrile that were infused directly into a Waters Quattro Micro mass spectrometer via an electrospray ion source as described in Huang et al. (2016). The LC-MS/MS analysis was performed with an Agilent 1100 HPLC in-line to the Quattro Micro mass spectrometer using mobile phase A (0.1% formic acid/0.01% trifluoroacetic acid/water) and B (0.1% formic acid/0.01% trifluoroacetic acid/acetonitrile) with a flow rate of 0.5 mL/minute. Compound elution was performed using a linear gradient of 0-16% B mobile phase over 16 minutes followed by 2 minutes of 95% B for a run time of 20 minutes. A post-column addition of 0.1% formic acid in acetonitrile was added via a peek tee at a flow rate of 100  $\mu\text{L}$ /minute. Scans for diagnostic fragment masses allowed for detection of each unique xanthine alkaloid as described previously in Huang et al. (2016).

### Statistical analysis

Correspondence analysis (Jackson 1997) was used to ordinate modern-day, ancestral, and mutated ancestral CS enzymes based upon relativized substrate preferences. Symmetric plots were used to visualize the results. Nonindependence of the enzymes and substrate preferences was determined ( $P < 0.05$ ) and total inertia was 1.05 for the analysis described in Fig. 3. The first two factors of the analysis accounted for a total of 85% of the inertia. Positions of enzymes along the x-axis in the symmetric plot are due to variation in methylation preference for xanthine (coordinates  $< -0.5$ ) or

3X (coordinates > 1). On the other hand, preference for 7X methylation is explained by position along the y-axis (coordinates < -0.5).

#### Data availability

Individuals interested in the data matrices underlying this article may obtain them upon request of the corresponding author. The original data underlying this article are available in <https://www.ncbi.nlm.nih.gov/genbank/> as well as <https://db.cngb.org/onekp/>.

#### Acknowledgements

This work was supported by National Science Foundation grant (MCB-1120624 to T.J.B.). Greg Cavey is thanked for assistance provided with LC-MS analyses. Ricky Stull and two anonymous reviewers provided helpful feedback on previous versions of the manuscript.

Table 1. Enzyme kinetic parameter estimates for modern-day and ancestral enzymes with selected substrates.

Enzyme (substrate)	$K_M$ ( $\mu\text{M}$ )	$k_{\text{cat}}$ (1/sec)	$k_{\text{cat}}/K_M$ ( $\text{s}^{-1}\text{M}^{-1}$ )
<b>Modern-day enzymes</b>			
TcCS1 (X)	95.80	8.37E-05	0.87
TcCS2 (3X)	49.10	9.81E-05	2.00
PcCS1 (X)	95.38	1.52E-03	15.94
PcCS2 (3X)	677.00	9.33E-04	1.38
<b>Ancestral enzymes</b>			
TcAncCS1 (X)	53.40	8.65E-05	1.62
TcAncCS1 (3X)	138.60	1.28E-04	0.92
TcAncCS1 (7X)	34.60	2.47E-04	7.20
TcAncCS2 (X)	4.14	3.39E-04	82.06
TcAncCS2 (3X)	154.00	3.32E-04	2.16
PcAncCS1 (X)	417.50	3.76E-04	0.90
CsAncCS (7X)	26.70	1.05E-03	39.33



## Figure Legends

Figure 1. The xanthine alkaloid biosynthetic network in plants potentially includes 12 unique paths leading from xanthosine and xanthine to caffeine. Ring nitrogen atoms are numbered on X and XR to show that the order in which N1, N3 and N7 are methylated differs between each pathway. Several of these appear to be utilized across angiosperms. Dotted arrows show the presumed pathway through which the majority of flux is achieved in *Coffea* using XMT-type enzymes and *Camellia* using CS-type enzymes. Dashed arrows show the presumed network utilized by *Citrus* which uses XMT-type enzymes. Solid thick and thin lines show the common pathway hypothesized for *Paullinia* and *Theobroma*, respectively, although the final step to caffeine from theobromine is unclear for the latter. Both *Paullinia* and *Theobroma* utilize CS-type enzymes to catalyze the reactions shown. Enzyme names are provided next to reactions they catalyze. Distinct structure colors are kept consistent with subsequent figures.

Figure 2. Substrate preferences of ancestral CS-type enzymes reveal the origins of modern-day enzyme activities. A. Estimated CS gene tree (lnL = -19220.31407) shows general relationships amongst sequences from divergent orders of angiosperms. Node labels are shown for reconstructed ancestral enzymes. B. Xanthine alkaloid substrates tested with each CS enzyme are color-coded to represent structures shown in Fig. 1. X=xanthine, XR=xanthosine, 1X=1-methylxanthine, 3X=3-methylxanthine, 7X=7-methylxanthine, TP=theophylline, TB=theobromine, PX=paraxanthine, CF=caffeine. C. Ancestral *Paullinia* CS enzymes preferred to methylate 7X as shown by the pie charts at nodes M & N but ultimately evolved modern-day enzymes to sequentially methylate X and 3X and catalyze a complete pathway to TB. D. Ancestral *Theobroma* CS enzyme at Node O preferred to methylate 7X. After duplication, preference for X evolved in the ancestral enzyme at Node P. From this enzyme, modern-day *Theobroma* CS enzymes evolved substrate preferences allowing for TB biosynthesis via sequential methylation of X and 3X. E. Ancestral *Camellia* CS



enzyme of Node Q also preferred to methylate 7X but later evolved divergent modern-day activities shown for *C. sinensis* TCS1 and TCS2. Inset boxes showing caffeine pathway network is shaded for ancestral enzymes. The pie charts of Fig. 2C-E represent mean relative activity with each substrate for the combined ancestral alleles at each node. Enzymes marked with “\*” are taken from published studies from other laboratories.

Figure 3. Ancestral CS enzymes experienced mutations to homologous regions and exhibited convergent changes in substrate preferences. A. Alignments in Region I and III of CS enzymes shows that both were mutated in ancestral *Theobroma* and *Paullinia* enzymes whereas only ancestral *Citrus* XMT (Huang et al. 2016) experienced substitution in Region II. Ancestral/derived amino acid states are shown in blue/red respectively. B. Correspondence analysis shows that ancient CS enzymes were similar and associate due to 7X methylation preference (node labels and substrate colors in pie charts taken from Fig. 2C-E). From these ancestral activities, convergent modern-day enzyme substrate preferences evolved largely by mutations to common protein regions. It appears that mutations to region I in PcAncCS2 and TcAncCS2 resulted in the convergent evolution of similar enzymes, PcCS2 & TcCS2, that associate due to preference to methylate 3X to form TB. Mutations to region III of PcAncCS2 and TcAncCS1 resulted in increased relative preference for X to form 3X and ultimately contributed to the convergent evolution of PcCS1 & TcCS1. Arrows between enzyme coordinates represent the enzyme lineages shown in Fig. 2.

## References

- Abascal F, Zardoya R, Posada D. 2005. ProtTest: selection of best-fit models of protein evolution. *Bioinformatics*. 21:2104-2105.
- Anaya AL, Cruz-Ortega R, Waller GR. 2006. Metabolism and ecology of purine alkaloids. *Front Biosci*. 11:2354-2370.
- Angelo PCSA, Nunes-Silva CG, Brigido MM, Azevedo JSN, Assuncao EN, Sousa ARB, Patricio FJB, Rego MM, Peixoto JCC, Oliveira WP, et al. 2008. Guarana (*Paullinia cupana* var. *sorbilis*),

an anciently consumed stimulant from the Amazon rain forest: the seeded-fruit transcriptome. *Plant Cell Rep.* 27:117-124.

Argout X, Fouet O, Wincker P, Gramacho K, Legavre T, Sabau X, Risterucci AM, Da Silva C, Cascardo J, Allegre M, et al. 2008. Towards the understanding of the cocoa transcriptome: Production and analysis of an exhaustive dataset of ESTs of *Theobroma cacao* L. generated from various tissues and under various conditions. *BMC Genomics.* 9.

Argout X, Salse J, Aury J-M, Guiltinan MJ, Droc G, Gouzy J, Allegre M, Chaparro C, Legavre T, Maximova SN, et al. 2011. The genome of *Theobroma cacao*. *Nat Genet.* 43:101–108.

Ashihara H, Crozier A. 2001. Caffeine: a well known but little mentioned compound in plant science. *Trends Plant Sci.* 6:407-413.

Ashihara H, Monteiro AM, Gillies FM, Crozier A. 1996. Biosynthesis of caffeine in leaves of coffee. *Plant Physiol.* 111:747-753.

Ashihara H, Sano H, Crozier A. 2008. Caffeine and related purine alkaloids: Biosynthesis, catabolism, function and genetic engineering. *Phytochemistry.* 69:841-856.

Ashihara H, Suzuki T. 2004. Distribution and biosynthesis of caffeine in plants. *Front Biosci.* 9:1864-1876.

Barkman TJ, Zhang J. 2009. Evidence for escape from adaptive conflict? *Nature.* 462:E1-2.

Baumann TW, Schulthess BH, Hanni K. 1995. Guaraná (*Paullinia cupana*) rewards seed dispersers without intoxicating them by caffeine. *Phytochemistry.* 39:1063-1070.

Bridgham JT, Carroll SM, Thornton JW. 2006. Evolution of hormone-receptor complexity by molecular exploitation. *Science.* 312:97-101.

Bridgham JT, Ortlund EA, Thornton JW. 2009. An epistatic ratchet constrains the direction of glucocorticoid receptor evolution. *Nature.* 461:515-519.

Chang BSW, Jonsson K, Kazmi MA, Donoghue MJ, Sakmar TP. 2002. Recreating a functional ancestral archosaur visual pigment. *Mol Biol Evol.* 19:1483-1489.

- Christin P-A, Weinreich DM, Besnard G. 2010. Causes and evolutionary significance of genetic convergence. *Trends Genet.* 26:400-405.
- Daly JW, Buttslamb P, Padgett W. 1983. Subclasses of adenosine receptors in the central nervous-system - interaction with caffeine and related methylxanthines. *Cell Mol Neurobiol.* 3:69-80.
- Dean AM, Thornton JW. 2007. Mechanistic approaches to the study of evolution: the functional synthesis. *Nature Rev Genet.* 8:675-688.
- Deng C, Xiuping K, Lin-Lin C, Si-an P, Limao F, Wei-Wei D, Zhao J, Zheng-Zhu Z. 2020. Metabolite and transcriptome profiling on xanthine alkaloids-fed tea plant (*Camellia sinensis*) shoot tips and roots reveal the complex metabolic network for caffeine biosynthesis and degradation. *Front Plant Sci.* 11:551288.
- Denoeud F, Carretero-Paulet L, Dereeper A, Droc G, Guyot R, Pietrella M, Zheng CF, Alberti A, Anthony F, Aprea G, et al. 2014. The coffee genome provides insight into the convergent evolution of caffeine biosynthesis. *Science.* 345:1181-1184.
- Des Marais DL, Rausher MD. 2008. Escape from adaptive conflict after duplication in an anthocyanin pathway gene. *Nature.* 454:762-U785.
- Des Marais DL, Rausher MD. 2010. Parallel evolution at multiple levels in the origin of hummingbird pollinated flowers in *Ipomoea*. *Evolution.* 64:2044-2054.
- Field SF, Matz MV. 2010. Retracing evolution of red fluorescence in GFP-like proteins from Faviina corals. *Mol Biol Evol.* 27:225-233.
- Figueiredo LC, Faria-Campos AC, Astolfi S, Azevedo JL. 2011. Identification and isolation of full-length cDNA sequences by sequencing and analysis of expressed sequence tags from guarana (*Paullinia cupana*). *Genet Mol Res.* 10:1188-1199.
- Gaucher EA, Govindarajan S, Ganesh OK. 2008. Palaeotemperature trend for Precambrian life inferred from resurrected proteins. *Nature.* 451:704-707.
- Granick S. 1957. Speculations on the origins and evolution of photosynthesis. *Ann Ny Acad Sci.* 69:292-308.



- Manceau M, Domingues VS, Linnen CR, Rosenblum EB, Hoekstra HE. 2010. Convergence in pigmentation at multiple levels: mutations, genes and function. *Philos T R Soc B*. 365:2439-2450.
- Mazzafera P, Wingsle G, Olsson O, Sandberg G. 1994. S-Adenosyl-L-methionine-theobromine 1-N-methyltransferase, an enzyme catalyzing the synthesis of caffeine in coffee. *Phytochemistry*. 37:1577-1584.
- McCarthy AA, McCarthy JG. 2007. The structure of two N-methyltransferases from the caffeine biosynthetic pathway. *Plant Physiol*. 144:879-889.
- Mizuno K, Kato M, Irino F, Yoneyama N, Fujimura T, Ashihara H. 2003. The first committed step reaction of caffeine biosynthesis: 7-methylxanthosine synthase is closely homologous to caffeine synthases in coffee (*Coffea arabica* L.). *Febs Lett*. 547:56-60.
- Mizuno K, Matsuzaki M, Kanazawa S, Tokiwano T, Yoshizawa Y, Kato M. 2014. Conversion of nicotinic acid to trigonelline is catalyzed by N-methyltransferase belonged to motif B' methyltransferase family in *Coffea arabica*. *Biochem Bioph Res Co*. 452:1060-1066.
- Mizuno K, Okuda A, Kato M, Yoneyama N, Tanaka H, Ashihara H, Fujimura T. 2003. Isolation of a new dual-functional caffeine synthase gene encoding an enzyme for the conversion of 7-methylxanthine to caffeine from coffee (*Coffea arabica* L.). *Febs Lett*. 534:75-81.
- Natarajan C, Hoffman FG, Weber RE, Fago A, Witt C, C., Storz JF. 2016. Predictable convergence in hemoglobin function has unpredictable molecular underpinnings. *Science*. 354:336-339.
- Nathanson JA. 1984. Caffeine and related methylxanthines - possible naturally-occurring pesticides. *Science*. 226:184-187.
- Olson-Manning CF. 2020. Elaboration of the corticosteroid synthesis pathway in primates through a multistep enzyme. *Mol Biol Evol*. 37:2257-2267.
- Pichersky E, Lewinsohn E. 2011. Convergent evolution in plant specialized metabolism. *Ann Rev Plant Biol*. 62:549-566.

- Schimpl FC, Kiyota E, Mayer JLS, Goncalves JFD, da Silva JF, Mazzafera P. 2014. Molecular and biochemical characterization of caffeine synthase and purine alkaloid concentration in guarana fruit. *Phytochemistry*. 105:25-36.
- Smith SD, Wang S, Rausher MD. 2012. Functional evolution of an anthocyanin pathway enzyme during a flower color transition. *Mol Biol Evol*. 30:602-612.
- Storz JF. 2016. Causes of molecular convergence and parallelism in protein evolution. *Nat Rev Genet*. 17:239-250.
- Suzuki T, Takahashi E. 1976. Caffeine biosynthesis in *Camellia sinensis*. *Phytochemistry*. 15:1235-1239.
- Suzuki T, Waller GR. 1987. Allelopathy Due to Purine Alkaloids in Tea Seeds during Germination. *Plant Soil*. 98:131-136.
- Taniguchi F, Fukuoka H, Tanaka J. 2012. Expressed sequence tags from organ-specific cDNA libraries of tea (*Camellia sinensis*) and polymorphisms and transferability of EST-SSRs across *Camellia* species. *Breed Sci*. 62:186-195.
- Thornton JW. 2004. Resurrecting ancient genes: experimental analysis of extinct molecules. *Nat Rev Genet*. 5:366-375.
- Uefuji H, Ogita S, Yamaguchi Y, Koizumi N, Sano H. 2003. Molecular cloning and functional characterization of three distinct N-methyltransferases involved in the caffeine biosynthetic pathway in coffee plants. *Plant Physiol*. 132:372-380.
- Uefuji H, Tatsumi Y, Morimoto M, Kaothien-Nakayama P, Ogita S, Sano H. 2005. Caffeine production in tobacco plants by simultaneous expression of three coffee N-methyltransferases and its potential as a pest repellent. *Plant Mol Biol*. 59:221-227.
- Wall PK, Leebens-Mack J, Muller KF, Field D, Altman NS, dePamphilis CW. 2008. PlantTribes: a gene and gene family resource for comparative genomics in plants. *Nucleic Acids Res*. 36:D970-D976.

- Wei C, Yang H, Wang S, Zhao J, Liu C, Gao L, Xia E, Lu Y, Tai Y, She G, et al. 2018. Draft genome sequence of *Camellia sinensis* var. *sinensis* provides insights into the evolution of the tea genome and tea quality. *Proc Natl Acad Sci USA*. 115:E4151–E4158.
- Wheeler LC, Smith SD. 2019. Computational modeling of anthocyanin pathway evolution: biases, hotspots, and trade-offs. *Integr Comp Biol*. 59:585-598.
- Wright GA, Baker DD, Palmer MJ, Stabler D, Mustard JA, Power EF, Borland AM, Stevenson PC. 2013. Caffeine in floral nectar enhances a pollinator's memory of reward. *Science*. 339:1202-1204.
- Yang Z. 2007. PAML 4: phylogenetic analysis by maximum likelihood. *Mol Biol Evol*. 24:1586-1591.
- Yoneyama N, Morimoto H, Chuang-Xing Y, Ashihara H, Mizuno K, Kato M. 2006. Substrate specificity of N-methyltransferase involved in purine alkaloids synthesis is dependent upon one amino acid residue of the enzyme. *Mol Genet Genomics*. 275:125-135.
- Zeng L, Zhang N, Zhang Q, Endress PK, Huang J, Ma H. 2017. Resolution of deep eudicot phylogeny and their temporal diversification using nuclear genes from transcriptomic and genomic datasets. *New Phytol*. 214.
- Zhang JZ. 2006. Parallel adaptive origins of digestive RNases in Asian and African leaf monkeys. *Nat Genet*. 38:819-823.
- Zubieta C, Ross JR, Koscheski P, Yang Y, Pichersky E, Noel JP. 2003. Structural basis for substrate recognition in the salicylic acid carboxyl methyltransferase family. *Plant Cell*. 15:1704-1716.

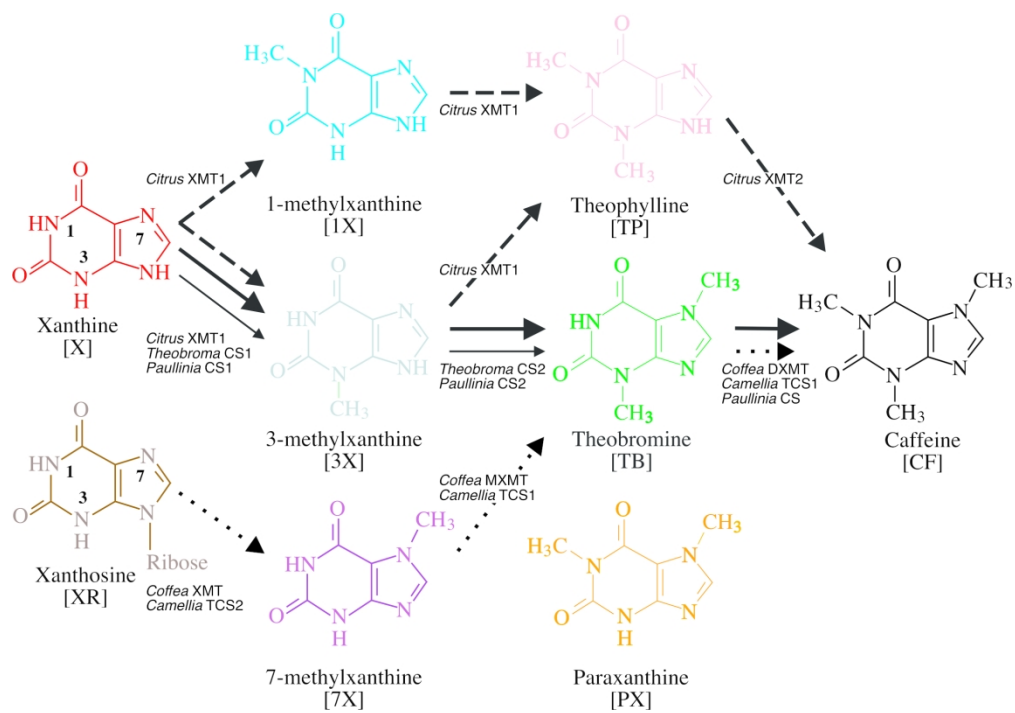


Figure 1

193x134mm (300 x 300 DPI)





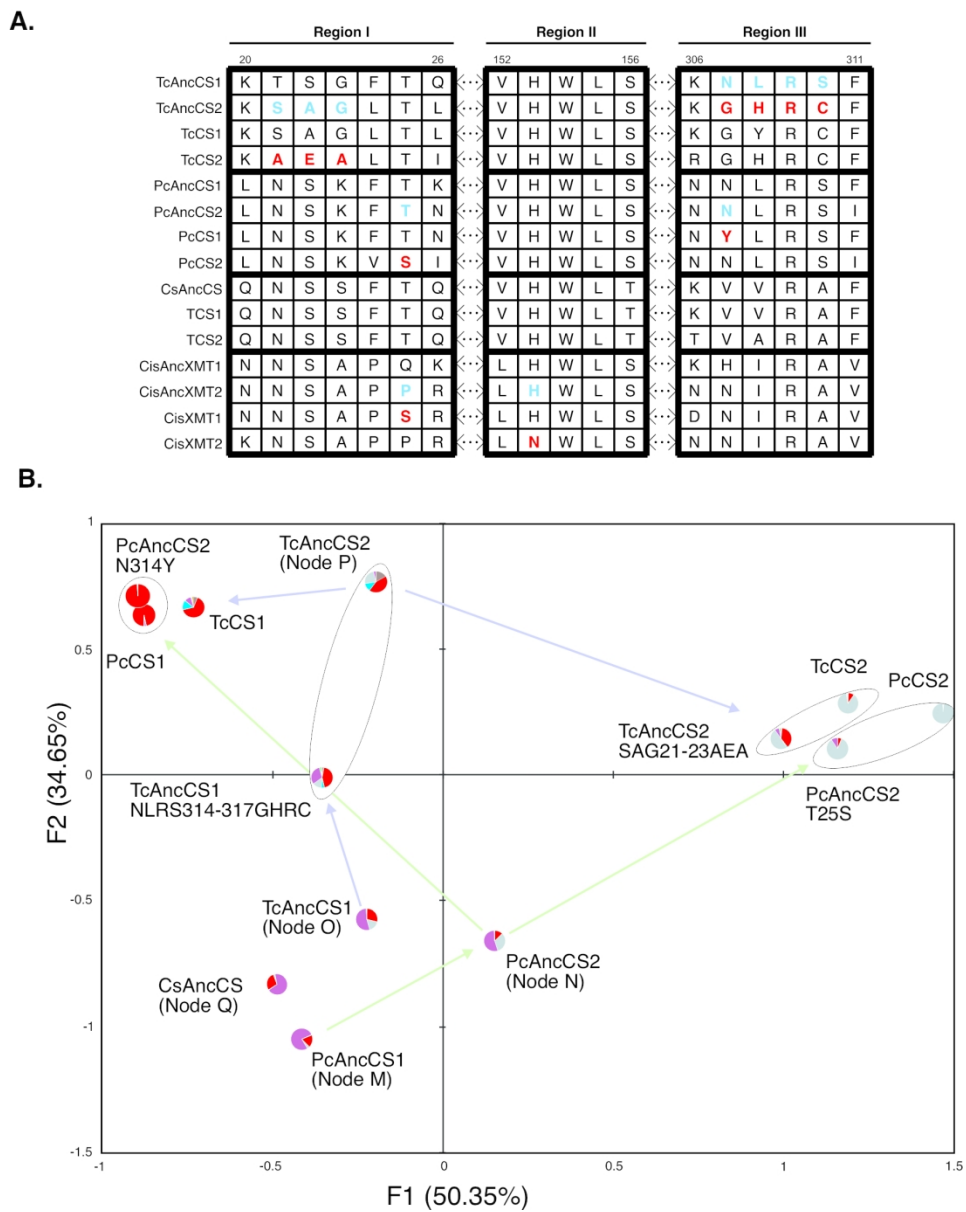


Figure 3

154x194mm (300 x 300 DPI)